PFC/JA-95-43

Theory of Hybrid Contact Discontinuities

A. Shajii and J.P. Freidberg

November 1995

Plasma Fusion Center
Massachusetts Institute of Technology
Cambridge, MA 02139 USA

Submitted for publication in: **Physical Review Letters**

This work was supported by the US Department of Energy under contract DE-FC02-93ER54186. Reproduction, translation, publication, use, and disposal, in whole or in part, by or for the US Government is permitted.

Abstract

This paper describes a new form of discontinuous solution for low Mach number flow of an ideal gas in a channel. The solution is best described as a "hybrid contact discontinuity", where in addition to jumps in temperature and density, the fluid velocity also develops a discontinuity across the moving contact surface. The pressure, however, remains continuous. It is shown that, in contrast to the standard contact discontinuity, the velocity of the contact surface does not equal, but is much slower than the gas velocity. The new features of the hybrid contact discontinuity result from the thermal interaction between the gas and the channel wall. Furthermore, it is conjectured that this interaction can result in stabilization of the contact surface against the expected Rayleigh-Taylor instability.

I. Introduction

This paper describes a new form of discontinuous fluid flow, referred to as a "hybrid contact discontinuity." The work is motivated by studies of quench propagation in long superconducting cables cooled by supercritical helium [1,2]. These studies have shown that the quench front exhibits many properties characteristic of a standard contact discontinuity: subsonic flow, jumps in density and temperature, but continuous pressure [3,4]. However, analysis of the thermal hydraulics model describing the system shows clearly that standard contact discontinuity solutions do not exist. The difficulty has been traced back to the presence of a channel wall, assumed to be in good thermal contact with the helium coolant. This recognition has led to the present study, which presents a somewhat simplified model of the quench problem, but which maintains all the salient physical effects.

In the course of the research, we have also discovered that similar models and phenomena are of interest to several other scientific fields. These include fluid flow in porous media [5,6,7], packed beds [8], and capillary tubes [7].

The main result of the research is the discovery of the hybrid contact discontinuity, a new form of discontinuous subsonic flow that includes the coupling effect between the gaseous coolant and the channel wall. There are three novel features to the flow. First, there is a velocity jump across the front, a phenomenon not observed in the standard contact discontinuity. As a result, the propagation velocity of the front is generally very different from the coolant velocity. Second, the structure of the expanding front is determined by the thermal conductivity of the channel, not the coolant. Third, on the basis of a reasonable conjecture, it is shown that, while the standard contact discontinuity is usually thought to be unstable to Rayleigh-Taylor type instabilities [9,10], the hybrid contact discontinuity can be stabilized by the presence of the channel wall.

These points are elucidated in the main body of the text.

II. Model

Consider the flow of an ideal gas through a circular cross-section channel [11]. The standard one dimensional model for the gas consists of the conservation of mass, momentum, and energy, and an equation of state. For the channel, only the conservation of energy is required. The model is given by

$$\frac{\partial \rho}{\partial t} + \frac{\partial}{\partial x}\rho v = 0 \tag{1}$$

$$\frac{\partial p}{\partial x} + \frac{f\rho v|v|}{4a} = 0 \tag{2}$$

$$\frac{3}{2}R\rho\left(\frac{\partial T}{\partial t} + v\frac{\partial T}{\partial x}\right) + \frac{\partial}{\partial x}(pv) = \frac{2h}{a}(T_w - T) \tag{3}$$

$$p = R\rho T \tag{4}$$

$$\rho_w C_w \frac{\partial T_w}{\partial t} = \frac{\partial}{\partial x}\left(\kappa_w \frac{\partial T}{\partial x}\right) + \frac{h}{b}(T - T_w)\ . \tag{5}$$

Note that for the low Mach number flows of interest, inertia is neglected in the momentum equation [11]. For turbulent flow we assume "fully rough" flow with $f \approx$ const. $= 0.07$, while for laminar flow $f = K/Re$ where $Re = 2\rho v a/\mu$ is the Reynolds number. For a circular channel $K = 64$, a is the channel radius, and b is the wall thickness (and we assume a thin wall: $b/2a \ll 1$).

The energy equation for the gas includes the effects of convection, compression, and viscous heating. Conduction is neglected since it is usually very small. In the channel wall, however, heat conduction must be maintained as this is the dominant effect determining the structure of the contact discontinuity (conduction in the channel wall is much larger than both thermal and viscous diffusion in the gas). For simplicity, κ_w and C_w are assumed to be constants.

The energy equations can be simplified by focusing on the interesting regime of high heat transfer $h \to \infty$. In this limit $(T_w - T) \to 0$. Adding Eqs. (3) and (5) and setting $T_w = T$ yields the following single hybrid energy equation

$$\left(\frac{3}{2}R\rho + \frac{2b}{a}\rho_w C_w\right)\frac{\partial T}{\partial t} + \frac{3}{2}R\rho v\frac{\partial T}{\partial x} + \frac{\partial}{\partial x}(pv) = \kappa_t \frac{\partial^2 T}{\partial x^2} \tag{6}$$

where $\kappa_t = (2b/a)\kappa_w$. The hybrid model thus consists of Eqs. (1), (2), (4) and (6).

The contact discontinuity is to be initiated into a steady state flow equilibrium described by this model. If one specifies the inlet pressure p_i, inlet temperature T_i, and outlet pressure p_o, it can be easily shown that the relations given below are an exact solution to the hybrid model for any $f = f(Re)$ [11].

$$p = p_i \left[1 - (1 - p_o^2/p_i^2)\,(x/L)\right]^{1/2} \tag{7}$$

$$T = T_i \tag{8}$$

$$\rho = \rho_i \left[1 - (1 - p_o^2/p_i^2)\,(x/L)\right]^{1/2} \tag{9}$$

$$v = \frac{v_i}{\left[1 - (1 - p_o^2/p_i^2)\,(x/L)\right]^{1/2}}\,. \tag{10}$$

Here, $\rho_i = p_i/RT_i$, $v_i = [2aRT_i(p_i^2 - p_o^2)/fLp_i^2]^{1/2}$, and L is the length of the channel.

III. The Contact Discontinuity Jump Conditions

Assume that at $t = 0$ the temperature at the inlet is suddenly raised from T_i to $\hat{T}_i$ while maintaining the original inlet pressure p_i. There is a corresponding decrease in density from ρ_i to $\hat{\rho}_i = p_i/R\hat{T}_i$. Temporarily setting aside the question of stability, one expects the temperature discontinuity to propagate along the channel with a velocity V_f. This velocity changes slowly with time in accordance with changes in the background state of the flowing gas. The width of the front spreads with time but on a much slower time scale.

In the case of negligible channel wall effects ($\rho_w = 0$) the picture above accurately describes the "standard" contact discontinuity. Two major results from the standard analysis are that the fluid velocity is always continuous across the front and that the front velocity is equal to the fluid velocity.

When the channel effects are not negligible the situation changes substantially. It is still possible to have a propagating front, but in this case the fluid velocity also develops a discontinuity and the front velocity has a value lower than the smaller value of v on either side of the front. This is one novel feature of the "hybrid" contact discontinuity.

These assertions are proven as follows. First, as is standard in the analysis of contact discontinuities, neglect the effect of thermal conduction. Second, assume the front moves with a velocity $V_f(t)$ and transform coordinates into the front reference frame: $z = x - \int V_f dt$. The jump conditions are obtained by assuming the existence of a discontinuity and integrating across the surface. The resulting conditions are given by

$$[\![\rho]\!] = -\rho_2 \frac{\Delta T}{T_1} \tag{11}$$

$$[\![p]\!] = 0 \tag{12}$$

$$[\![v]\!] = \frac{\alpha}{1+\alpha} \frac{\Delta T}{T_2} v_2 \tag{13}$$

$$V_f = \frac{v_2}{1+\alpha} \tag{14}$$

where $\alpha = (4b/5a)\rho_w C_w/(\rho_2 R)$ and $\Delta T = T_1 - T_2$. Here the subscripts "1" and "2" denote the regions behind and ahead of the front, respectively. Also $[\![Q]\!]$ denotes $Q_1 - Q_2$ and $z = 0$ is the front location, corresponding to $X_f(t) = \int V_f dt$. To interpret these relations assume that the fluid conditions are known just ahead of the front (0^+) in the unperturbed region and that the temperature T_1, related to $\hat{T}_i$, is specified just behind the front (0^-). A short calculation then determines the values of all other quantities behind the front. In the limit of no channel ($\rho_w = 0$) it immediately follows that $[\![p]\!] = [\![v]\!] = 0$, $V_f = v$, and $[\![\rho]\!] = -\rho_2(\Delta T/T_1)$. This is the standard contact discontinuity [3,4].

Observe that for the general case with a channel wall (i.e. $\rho_w \neq 0$) the fluid velocity develops a discontinuity across the front. (Note that in this case the jump in pressure is actually $[\![p]\!] \sim O(M^2)$, where M is the Mach number. However, to zeroth order where inertia is ignored this jump is negligible.) Furthermore, the front velocity decreases as the wall contribution α increases. It can easily be shown that $V_f < v_2 < v_1$ for $\Delta T > 0$ (a rise in inlet temperature) and $V_f < v_1 < v_2$ for $\Delta T < 0$. The discontinuity in the velocity

results from the "thermal drag" caused by the channel wall. For the case $T_1 > T_2$, as the high temperature gas at T_1 initially flows past the front, it encounters the wall which is at $T = T_2$. Thus, a heat exchange takes place between the gas and the wall. As a result of this heat transfer, the gas heats the wall just ahead of the "old" front to $T = T_1$, creating a "new" front. After the gas has passed the new front it has cooled to $T = T_2$. During this cooling process the gas density increases to maintain a continuous pressure; therefore, the velocity decreases to maintain a continuous mass flow in the frame of the front. As a final point note that the jump conditions do not depend on the specific properties of the friction factor.

The conclusion is that in the combined fluid-channel system, subsonic hybrid contact discontinuities can propagate, and are characterized by a continuous pressure and discontinuous temperature, density and velocity.

IV. Numerical Solution

This section presents the results of a non-linear, time dependent numerical solution of the hybrid model described by Eqs. (1),(2),(4) and (6). The purpose is twofold. First, the numerical solution provides further, more complete proof of the existence of the hybrid contact discontinuity. Second, an examination of the numerical results yields physical insight that can be used to construct a purely analytical solution.

We have carried out many such numerical simulations. For the sake of presentation we select a set of parameters that are typical of a large superconducting fusion magnet using helium as the coolant, keeping in mind that the use of the ideal gas model is an obvious oversimplification of the actual situation. The parameters of interest are given by $p_i = 0.8$ MPa , $p_o = 0.4$ MPa, $T_i = 100$ K, $b = 0.1$ mm, $a = 0.5$ mm, $L = 100$ m, $\rho_w = 8000$ kg/m^3, $C_w = 350$ J/kg-K, $\kappa_w = 10$ W/m-K, $f = 0.07$, $\rho_i = 3.85$ kg/m^3, $R = 2080$ J/kg-K, corresponding to $v_i = 4.25$ m/s.

The stationary flow solution given by Eqs. (7)-(10) is used as an initial condition. At time $t = 0^+$ the inlet temperature is suddenly raised to the value $\hat{T}_i = 200$ K, keeping the

inlet pressure fixed. The resulting time evolution is illustrated in Fig. 1. Plotted here are curves of T, v, and p versus x for various values of time.

The following points are apparent. The initial inlet temperature discontinuity propagates along the channel with a nearly uniform, highly subsonic velocity ($V_f \approx 0.075$ m/s, while the speed of sound at the inlet is ≈ 590 m/s). There is a thin transition region which maintains its boundary layer structure as the front progresses; if there is spreading of the front it is occurring on a much slower time scale than the typical front propagation time. During the evolution the pressure remains continuous across the front. The solutions on either side of the front are quite similar to the steady flow solutions although with different parameters in each region.

As predicted in Section III, the fluid velocity also develops a discontinuity across the front, a unique characteristic of the hybrid contact discontinuity. From the curves corresponding to $t = 200$ s observe that $V_f \approx 0.075$ m/s, $v_1 \approx 8.4$ m/s, $v_2 \approx 4.4$ m/s, thereby confirming the previously derived velocity inequality $V_f < v_2 < v_1$. A careful measurement of the fluid variables on each side of the front also shows that the hybrid jump conditions are satisfied both qualitatively and quantitatively. The conclusion from the numerical studies is that long lived, propagating hybrid contact discontinuity exits as implied by the simple jump condition analysis.

V. Analytical Solution

The next step is to develop an analytical theory of the hybrid contact discontinuity. The theory provides valuable scaling information and allows us to make a highly plausible conjecture concerning the stability of the front. The analysis has the structure of a classic boundary layer problem. A small parameter, related to the thermal conductivity, is identified which leads to a simplified set of equations for the front in terms of the "stretched" coordinates. This solution is then asymptotically matched to the "outer" regions in which the thermal conductivity can be neglected.

We proceed as follows. Consider first the boundary layer region corresponding to the front. Straightforward dimensional analysis in terms of the macroscopic lengths and

velocities shows that the small dimensionless parameter related to the thermal conductivity is given by $\epsilon = \sqrt{fT_i/4RLa}\,(\kappa_t/p_i)$. For the test case illustrated in Fig. 1, $\epsilon \approx 1.6\times10^{-6} \ll 1$. The layer analysis begins by transforming to the frame of the moving front. Next, stretched coordinates are introduced: $z' = z/\epsilon$ and $t' = (t - t_0)/\epsilon$ where t_0 is the current value of "unstretched" time. A simple calculation shows that in the layer region all terms in the model are of comparable order and must be retained except for the friction term in the momentum equation which is negligible.

It is worth noting that there are no steady state state solutions (in the moving frame) which asymptotically match to $T(z' \to -\infty) = T_1$ and $T(z' \to +\infty) = T_2$. The steady state solutions diverge as $z' \to +\infty$. Thus, the structure of the front is not invariant with time. The resolution of this problem is that the width of the front expands with time, a behaviour that can be well modelled by a similarity solution. An examination of the layer equations indicates that the appropriate similarity variable is given by $\xi = z'/\sqrt{Dt'}$, where the diffusion coefficient $D = \kappa_t/R\rho_2$ and $\rho_2 = \rho(z' \to +\infty)$.

In terms of ξ the layer equations reduce to

$$\frac{dU}{d\xi} + \left(\frac{\xi}{2} - U\right)\left(\frac{1}{T}\frac{dT}{d\xi}\right) = 0 \tag{15}$$

$$\frac{d^2T}{d\xi^2} + \frac{5}{2}T_2\left[\left(1 + \alpha\frac{T}{T_2}\right)\frac{\xi}{2} - U\right]\left(\frac{1}{T}\frac{dT}{d\xi}\right) = 0 \tag{16}$$

$$p = p_f = const. \tag{17}$$

Here, the velocity is related to U by $v = V_f\,(1 + \alpha T/T_2) + \sqrt{D/\epsilon t'}\;U$. Note that the pressure is continuous across the layer and that there is a jump in velocity proportional to the jump in temperature when $\rho_w \neq 0$. The matching conditions are $T(\xi \to -\infty) = T_1$, $T(\xi \to +\infty) = T_2$ and $U(\xi \to \pm\infty) = 0$. At this point $p_f(t_0)$ and $V_f(t_0)$ are as yet undetermined functions of the "unstretched" time.

The solution to Eqs. (15) and (16) can be shown to have the correct asymptotic behavior as $\xi \to \pm\infty$; that is, there always exists a solution to these equations which satisfies the matching conditions at $\xi \to \pm\infty$. An explicit analytic solution showing this

behavior can be obtained in the limit of small $(T_1 - T_2)/(T_1 + T_2)$ and is given by

$$T \approx \frac{1}{2}\left[T_1 + T_2 - (T_1 - T_2)\ erf(k\xi)\right] \tag{18}$$

$$U \approx \frac{1}{2\sqrt{\pi}}\left(\frac{T_1 - T_2}{kT_2}\right) e^{-k^2\xi^2} \tag{19}$$

where $k^2 = (5/8)(1 + \alpha)$. A simple calculation also shows that the layer solutions automatically satisfy the exact hybrid contact discontinuity jump conditions described by Eqs. (11)-(14).

These two results, the asymptotic matching at $\xi \to \pm\infty$ and the self consistency with the jump conditions demonstrates the existence of a moving front with proper mathematical and physical structure.

The second part of the analysis consists of determining the solutions in the outer regions and then matching across the front. The matching conditions ultimately determine the front velocity as a function of time in terms of the inlet and outlet boundary conditions. This is the desired goal. The outer solutions are obtained as follows. We transform back to the laboratory frame and re-introduce the original unstretched coordinates. In the limit of small ϵ all terms in the hybrid model are of comparable order and must be retained except for the thermal conduction term which is negligible.

The model at this point is a set of one dimensional plus time partial differential equations. A great simplification arises by observing from the numerical results that at any instant of time the solutions closely resemble the steady state solutions given by Eqs. (7)-(10). The parameters are different on each side of the front and evolve slowly in time. The time dependence results from the fact that the front velocity slowly varies due to the spatial dependence of the unperturbed gas as the front propagates along the channel. Using this insight we obtain approximate solutions in the outer regions by neglecting the time derivative terms. Time now appears only as a parameter. (We shall verify a posteori that the velocity does indeed evolve slowly.)

Under this assumption the solution behind and ahead of the front satisfying the inlet and outlet conditions can be written as

behind the front	ahead of the front	
$T = \hat{T}_i$	$T = T_i$	(20)
$p = p_i \left[1 - (\hat{v}_i^2/\eta\hat{v}^2)y\right]^{1/2}$	$p = p_o \left[1 + (\hat{v}_o^2/\eta\hat{v}^2)(1-y)\right]^{1/2}$	(21)
$v = \hat{v}_i \left[1 - (\hat{v}_i^2/\eta\hat{v}^2)y\right]^{-1/2}$	$v = \hat{v}_o \left[1 + (\hat{v}_o^2/\eta\hat{v}^2)(1-y)\right]^{-1/2}$.	(22)

Here, $y = x/L$, $\eta = \hat{T}_i/T_i$, $\hat{v}^2 = 2aRT_i/fL$ and $\hat{v}_i$, $\hat{v}_o$ are unknown parameters to be determined from the matching conditions.

The non-trivial matching conditions require that the pressure and velocity connect in the correct asymptotic manner with the layer solutions. These conditions give four relations for the unknowns $V_f(t)$, $p_f(t)$, $\hat{v}_i(t)$, $\hat{v}_o(t)$. After eliminating $\hat{v}_i$ and $\hat{v}_o$ we obtain a single equation for p_f and a subsidiary relation for V_f given by

$$\frac{dp_f}{d\tau} = \frac{(F+G)^{5/2}}{GF' - FG'} \tag{23}$$

$$V_f = \hat{v}\,(F+G)^{1/2} \tag{24}$$

where $\tau = \hat{v}t/L$, prime denotes d/dp_f, $\alpha_0 = (4b/5a)\rho_w C_w T_i/p_i$, and $F = \eta(p_i^2 - p_f^2)/(p_f + \alpha_0\eta p_i)^2$, $G = \left(p_f^2 - p_o^2\right)/(p_f + \alpha_0 p_i)^2$. After some analysis, one can derive an accurate approximation for the solution to Eq. (24), which can be written as

$$V_f(\tau) = V_{f0}\left(1 - \frac{3}{V_{f0}}\,\frac{dV_{f0}}{d\tau}\,\tau\right)^{-1/3} \tag{25}$$

Here,

$$V_{f0} = V_f\Big|_{\tau=0} = \frac{\hat{v}\left(1 - p_o^2/p_i^2\right)^{1/2}}{(1+\alpha_0)}$$

$$\frac{1}{V_{f0}}\,\frac{dV_{f0}}{d\tau} = \frac{1}{V_f}\,\frac{dV_f}{d\tau}\Big|_{\tau=0} = \frac{\left(1 - p_o^2/p_i^2\right)^{1/2}}{2\,(1+\alpha_0)}\left[1 - \left(\frac{1+\eta\alpha_0}{1+\alpha_0}\right)^2 \frac{p_o^2/p_i^2 + \alpha_0}{\eta\,(1+\alpha_0)}\right]$$

To test the theory the front velocity versus time as calculated from Eq. (25) and from the full non-linear hybrid model are compared in Fig. 2 for several values of α_0 for fixed $\hat{T}_i/T_i = 2$ and $p_o/p_i = 5/8$ (all the parameters are the same as the case presented

in Fig. 1 and only b is varied to obtained the required value of α_0). Observe that the agreement is quite good. Also, the velocity is a slowly varying function of time thereby justifying our neglect of the time derivatives in the analytical solutions. We conclude that the analytical theory is an accurate representation of the exact solution and thus contains all the important scaling information.

VI. Stability Conjecture

An important issue relating to the observability of contact discontinuities is whether or not the propagating front is stable. It has long been thought that such fronts are unstable to Rayleigh-Taylor type instabilities [4,9,10]. The simplest unstable case of a density jump contact discontinuity corresponds to a heavy fluid supported by a light fluid against the force of gravity. In more general terms Rayleigh-Taylor instabilities are expected whenever $\rho' g_{eff} < 0$, where g_{eff} is the effective acceleration felt by the front and $\rho' = \partial\rho/\partial x$ [4].

In this context, the solution for V_f given by Eq. (25) leads to the following conjecture regarding the stability of hybrid contact discontinuities. In the reference frame moving with the discontinuity the acceleration felt by the front is $g_{eff} = -dV_f/dt$. Consequently, when $\eta > 1$, the density gradient is positive and we expect instability when $dV_f/dt > 0$. Similarly, for $\eta < 1$, the density gradient is negative and instability should occur for $dV_f/dt < 0$. This is our basic conjecture.

The conditions for stability can then be easily calculated from Eq. (25) and are given by

$$
\begin{aligned}
1 > \eta &> \frac{1}{2\alpha_0}\left[A - \left(A^2 - 4A\right)^{1/2}\right] - \frac{1}{\alpha_0} \\
\eta &> \frac{1}{2\alpha_0}\left[A + \left(A^2 - 4A\right)^{1/2}\right] - \frac{1}{\alpha_0} \qquad (26) \\
A &= \frac{\left(1+\alpha_0\right)^3}{\alpha_0\left(\alpha_0 + p_o^2/p_i^2\right)}
\end{aligned}
$$

A plot of α_0 versus η for $p_o/p_i = 5/8$ is illustrated in Fig. 3. Consider first the incompressible limit, obtained by letting $p_o/p_i \to 1$. In this case the width of the stable band in η shrinks to zero and the stability boundary approaches a nearly horizontal line ($\alpha_0 = 1/\sqrt{\eta}$). Below this line, corresponding to a small wall effect, the front is unstable for all values of η. This is the traditional picture of the contact discontinuity stability. For larger values of α_0, however, the acceleration changes sign indicating that a sufficiently large wall effect can stabilize the front. The situation is qualitatively similar for the compressible case. The one new feature is the opening of a stability window even with no wall (i.e. $\alpha_0 = 0$) when $\eta < 1$ representing a negative temperature decrement at the inlet. The possibility of stabilization by means of a wall is another novel feature of the hybrid contact discontinuity.

VII. Conclusions

We have demonstrated the existence of a new form of contact discontinuity (hybrid contact discontinuity). The fluid flow in this regime is characterized by low Mach number, discontinuous velocity as well as density and temperature, an expanding front width, and a possible stabilization by means of interaction with a channel wall.

Acknowledgements

The authors would like to thank Professor R. Betti for several very useful discussions. This work was partially supported by the Office of Fusion Energy in the Department of Energy.

References

[1] A. Shajii, and J. P. Freidberg, J. Appl. Phys. **76**, 3149 (1994).

[2] A. Shajii, and J. P. Freidberg, J. Appl. Phys. **76**, 3159 (1994).

[3] L. D. Landau, and E. M. Lifshitz *Fluid Mechanics* (Pergamon Press, New York, 1987), pp. 320-321.

[4] G. Rudinger *Nonsteady Duct Flow Wave-Diagram Analysis* (Dover Publications, New York, 1969), pp. 87-88.

[5] R. E. Kidder, and X. X. La Habra, J. Appl. Mech. **24**, 329 (1957).

[6] F. A. Morrison, Ind. Eng. Chem. Fundam. **11**, No. 2, 191 (1972).

[7] M. Kaviany *Principles of Heat Transfer in Porous Media* (Springer-Verlog, New York, 1991).

[8] E. A. Foumeny, and J. Ma, Chem. Eng. Technol. **17**, 50 (1994).

[9] G. I. Taylor, Proc. Roy. Soc. A **201**, 193-196 (1950).

[10] D. J. Lewis, Proc. Roy. Soc. A **117**, 81-96 (1950).

[11] A. Shajii, and J. P. Freidberg, MIT Plasma Fusion Center Report, PFC/JA-95-5, 1995 (to be published in J. Fluid Mech.).

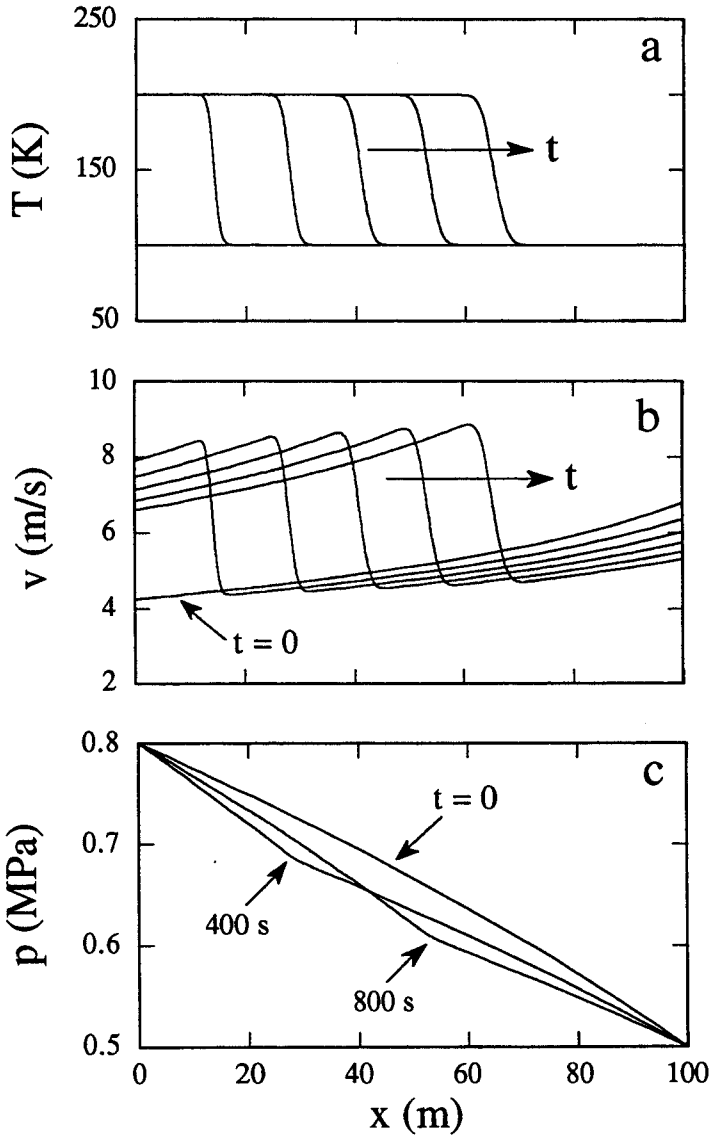

Figure 1: Temperature (a), velocity (b), and pressure (c) profiles along the channel at various times. The time intervals in figures a and b are 200 s.

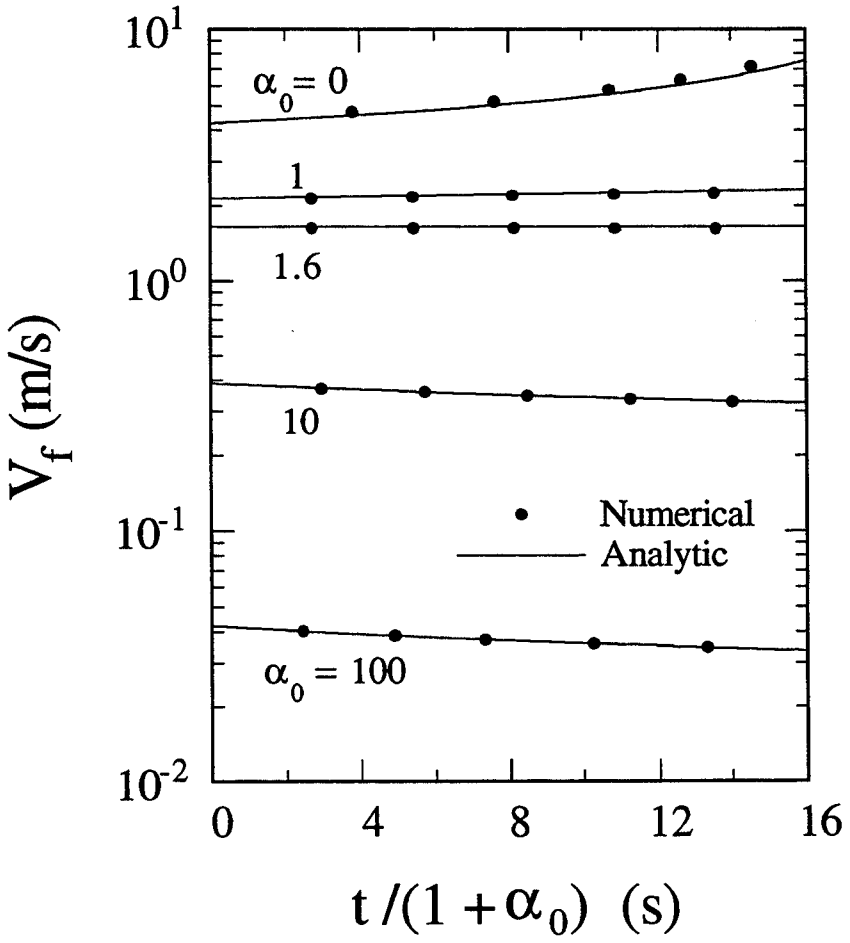

Figure 2: Front propagation velocity versus time for various values of α_0. The case $\alpha_0 = 1.6$ corresponds to the stability boundary ($dV_f/dt = 0$).

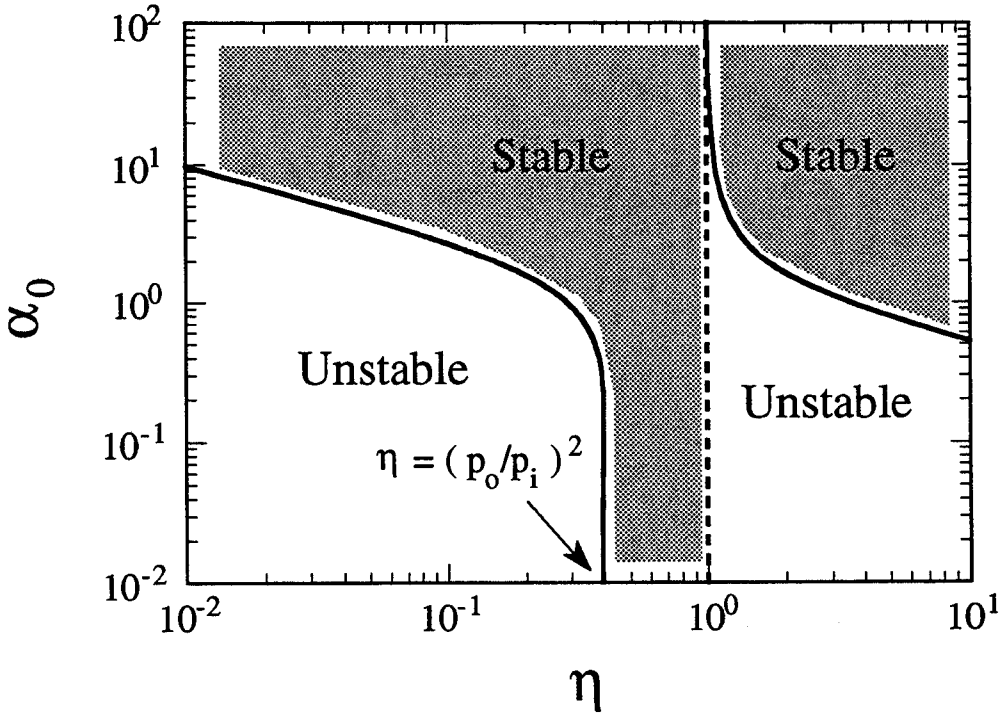

Figure 3: Stability curve for $p_o/p_i = 5/8$.